A Novel Axial-Flux-Complementary Doubly Salient Machine With Boosted PM Utilization for Cost-Effective Direct-Drive Applications

SHUANGXIA NIU[1], **(Senior Member, IEEE), XING ZHAO**[1],
XIAODONG ZHANG[2], **AND TIANTIAN SHENG**[1]

[1]Department of Electrical Engineering, The Hong Kong Polytechnic University, Hong Kong
[2]Shenzhen In Drive Amperex Company Ltd., Shenzhen 518052, China

Corresponding author: Xiaodong Zhang (xiaodong@eee.hku.hk)

ABSTRACT This paper proposes a novel axial-flux-complementary doubly salient machine (AFC-DSM) for cost-effective direct-drive applications. The key is to coordinate two complementary rotors with inset stator permanent magnets (PMs) circumferentially magnetized to construct an axially complementary flux return path in machine. Different from the traditional stator-PM machines, the excitation flux is transferred between the complementary rotors, hence switched smoothly without been shorted or opened in the air gaps. As a result, the PM utilization in the proposed machine can be doubled compared to that in traditional stator PM machine. In addition, the proposed machine also contributes to reduced cogging torque, higher winding utilization factor and neglectable mutual inductance, which helps to improve its torque performance as well as fault-tolerant capability. The electromagnetic performance is evaluated by 3-D finite element analysis, and the simulation results verify the effectiveness of the proposed machine.

INDEX TERMS Axial-flux-complementary, doubly salient machine, permanent magnet utilization.

I. INTRODUCTION

With the increasing concerns of environment pollution and energy consumption, powertrain electrification is a popular trend to reduce the use of nonrenewable petroleum [1]–[4]. Axial-flux permanent magnet machines are very suitable as direct-drive solutions for powertrain electrification due to their inherent advantages such as short axial dimension, high torque density and high efficiency [5]. Currently, most of disc axial-flux machines adopt PMs on the rotor, which helps improve the air-gap flux density [6]–[8]. However, PMs located on the rotor also cause some disadvantages for some direct-drive applications. For example, PMs on the rotors increase risk of damage due to the heavy bumps and vibrations experienced by the rotary parts. Also, the speed range of rotor-PM machines is almost limited, since the excitation flux density is high, and hence not easy to weaken the excitation flux by armature reaction.

The associate editor coordinating the review of this manuscript and approving it for publication was Xiaodong Sun.

To improve the robustness of direct-drive machines, many stator-PM axial flux machines are investigated, such as flux switching permanent machines (FSPMs), doubly salient permanent machines (DSPMs) and switch reluctance machines (SRMs) [9]–[13]. Different from DSPMs or SRMs, FSPMs have "C" core stator teeth and have PMs sandwiched between the cores [14], [15]. Obviously, the volume for PM in flux switching machine is much larger than the other stator-PM machines and contributes to stronger excitation field. In addition, it is noticed that the stator has been separated into many pieces, so the manufacturing difficulty for this kind of machines is much larger than others. For axial-flux FSPMs, the torque is relatively high because of the large usage of PMs and the magnetic congregating effect. However, the cost with the large amount of PM usage is also increased. Especially the utilization rate of the PMs is relatively low, since the excitation flux linkage is shorted and flux leakage is high when the rotor tooth is aligned to the PM.

DSPMs have pieces of PMs installed in the stator yoke and applies concentrated windings [16], [17]. The rotor adopts

simple laminations without PM or windings, which is low-cost and robust, so this kind of machines can endure severe vibrations. the major disadvantage for traditional DSPMs is the asymmetric flux path, which is the inherent characteristic of double salient machines. Since there are three stator teeth between the adjacent PMs, the distance from PMs to each stator teeth could not be even. This causes the asymmetric back-EMF and inductance for three phases, making great harmonics for the output torque. It worth mentioning that in some novel DSPMs, the asymmetric magnetic path is avoid [18]. However, the excitation flux switching way is different from the traditional double salient machines, which makes them sacrifice the torque density or PM utilization [19]–[21]. For axial-flux DSPMs, the space for PM is limited and the Back-EMF is not sinusoidal due to the asymmetrical magnetic path, so these machines have limited torque density and also very large torque ripple. For non-PM axial SRMs, although the cost is low, the relative lower torque density is the major drawbacks for such kind of machines.

To trade off the cost and torque density, a novel disc machine with flux dual complementary structure is proposed. This paper is organized by following. In Section II, the topology and operation principle of this proposed machine is introduced, and then its major characteristics are simulated with finite element methods in Section III. Section IV gives the evaluated electromagnetic performances and Section V presents the conclusion.

II. MACHINE CONFIGURATION AND OPERATION PRINCIPLE

A. MACHINE STRUCTURE

The topology of the proposed flux-dual-complementary axil-flux machine is shown in Fig.1. The stator has 24 slots with PMs installed in the yoke. The PMs are magnetized along circumferential direction and the adjacent ones are magnetized with the opposite directions. The rotor applies dual complementary structure, which means double rotors are adopted, which are staggered by 180° mechanical degrees. Each rotor has 11 salient teeth which vary the reluctance along the air-gap. The coils are wound around the stator teeth with the concentrated distribution, as shown in Fig. 1(b).

The proposed machine has salient advantages and very suitable for in-wheel applications in electric vehicle.

(1) The excitation flux path is specially designed with a dual complementary flux path, so the excitation flux can be switched smoothly without been shorted or opened, which helps to reduce the flux leakage and improve the PM utilization.

(2) Meanwhile, the PMs are inset within the stator yoke, the structure of which is reliable and robust compared to rotor PM design, and PMs can endure severe vibrations during operation.

(3) The concentrated winding distribution can reduce the end windings and reduce the copper losses, hence improving the efficiency of machine.

(a)

(b)

(c)
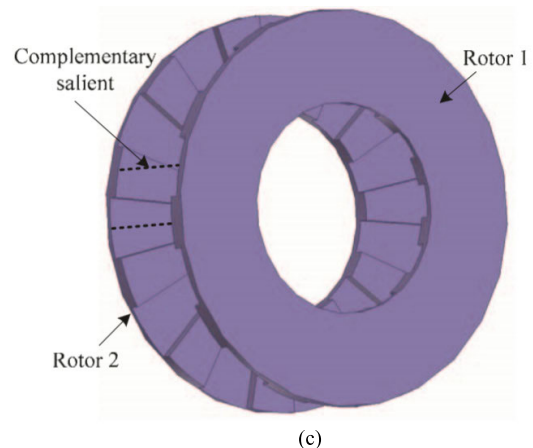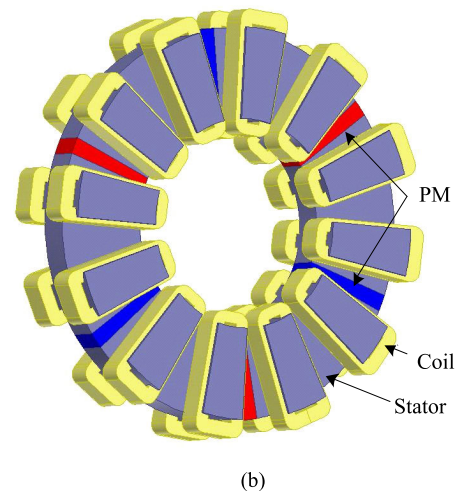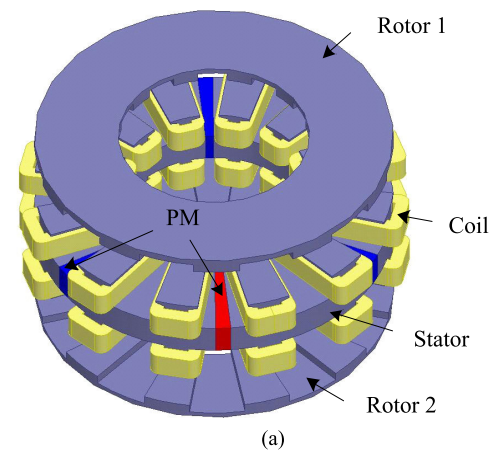
FIGURE 1. Topology of the proposed axial-flux-complementary doubly salient machine. (a) Overview of machine. (b) Stator with complementary inset PMs. (c) Complementary rotors.

(4) The complementary flux design also enables this machine to enhance the torque per PM amount as well as reduce the torque ripples and also obtain an improved performance in terms of the torque, efficiency and cost.

(5) Benefiting from the dual rotor structure, the axial force in two air gaps can be balanced, and thus the

synthetic force on bearings is zero, which accordingly reduces the possible vibration in axial direction and thus increases machine mechanical reliability.
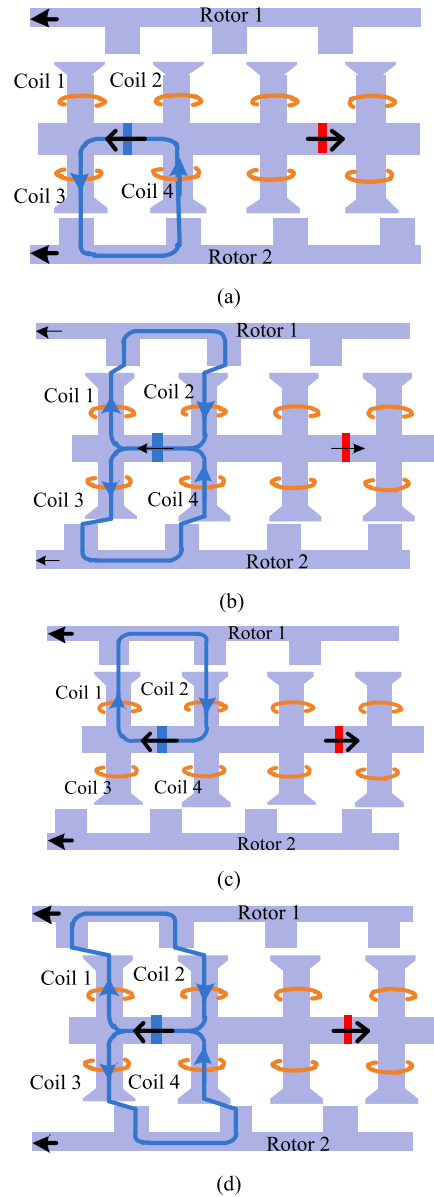
B. OPERATION PRINCIPLE

The operation principle of this machine is shown in Fig. 2. When the rotors move to 0° electrical degree as shown in Fig. 2(a), the excitation flux created by the PM would go through Coil 3, Rotor 2 and Coil 4 to form the close magnetic path. Ideally, there should be no excitation flux in Coil 1 and Coil 2, due to the relatively large magnetic reluctance. After that, as shown in Fig. 2(b), when the rotors move to 90° electrical degrees, the PM flux goes through the double rotors and passes through four coils. Next step, when the rotor moves to 180° electrical degrees, the PM flux goes through Coil 1, Rotor 1 and Coil 2, which is opposite to the magnetic path in Fig. 2(a). Next, when the rotors move to 270° electrical degrees, the flux goes through both sides again. During this cycle, the flux in Coil 3 and Coil 4 changes from the maximum value to zero and then back to the maximum, while the flux in Coil 1 and Coil 2 experiences zero to the negative maximum and back to zero.

There are two distinguished characteristics for this machine due to this dual complementary flux design. Firstly, the PM flux is switched smoothly from one group of coils to another complementary coil group in the whole period, without been shorted or opened. Therefore, the PM utilization factor could be improved. Secondly, the armature flux is parallel with the PM flux. Specifically, when the rotor moves to the position in Fig. 2(b) and Fig. 2(d), the drive current should get peak since the open-circuit back-EMF gets its maximum. At these positions, the armature flux goes through the stator and rotor teeth to form a circuit, instead of going through the PMs. This characteristic can increase the armature reaction to expand the flux weakening ability and torque speed range, and meanwhile avoid PM demagnetization.
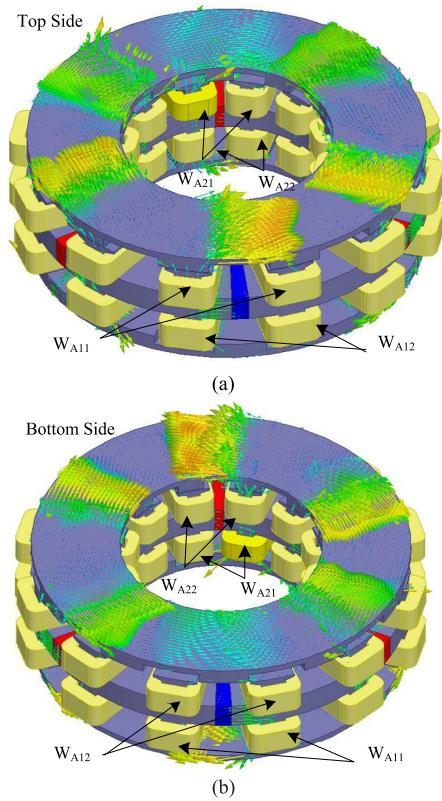
III. CHARACTERISTICS OF THE PROPOSED MACHINE

A. DUAL COMPLEMENTARY CHARACTERISTICS

As introduced in Section II, the most important feature of this machine is the dual complementary structure. To reveal this feature, the winding for phase A is taken for example. Eight coils belonging to winding A is divided into four sub-windings, namely W_{A11}, W_{A12}, W_{A21} and W_{A22}, as shown in Fig. 3. W_{A11} and W_{A21} are in upper layer while W_{A12} and W_{A22} are in lower layer. W_{A11} and W_{A12} are wound on the teeth besides PM with clockwise magnetization direction, while W_{A21} and W_{A22} are wound on the teeth besides the one with opposite magnetization direction. Dual complementary feature refers to 1) the excitation flux in the windings belonging to different layers is complementary, specifically, W_{A11} and W_{A12}, W_{A21} and W_{A22}, 2) the excitation flux in the windings besides PMs with opposite magnetization is complementary, for example W_{A11} and W_{A21}, W_{A12} and W_{A22}.

FIGURE 2. Operation principle diagram of the proposed machine. (a) Rotor at 0° electrical degree. (b) Rotor at 90° electrical degree. (c) Rotor at 180° electrical degree. (d) Rotor at 270° electrical degree.

Fig. 3 presents the simulation results of open-circuit flux distribution for this machine to demonstrate the dual complementary characteristic. Fig. 3(a) and Fig. 3(b) gives the flux distribution for top side and bottom side respectively. Comparing these two pictures, it is found that the excitation flux in W_{A11} (referred as ψ_{A11}) and in W_{A12} (referred as ψ_{A12}) is complementary, as ψ_{A11} gets maximum, ψ_{A12} gets minimum. So is the excitation flux in W_{A21} (written as ψ_{A21}) and in W_{A12} (written as ψ_{A12}). This is caused by the complementary rotor, as the reluctance along the air-gap under these windings is complementary. This characteristic brings one significant advantage, as the PM flux could switch smoothly between the upper layer and lower layer without been shorted or opened, which could improve the PM utilization factor.
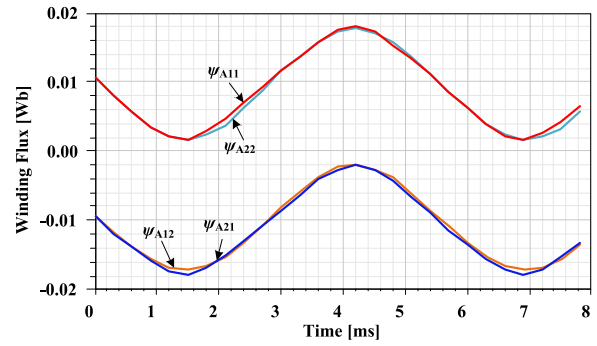
Top Side

W_{A21} W_{A22}

W_{A11} W_{A12}

(a)

Bottom Side

W_{A22} W_{A21}

W_{A12} W_{A11}

(b)

FIGURE 3. Open-circuit flux distribution of the proposed machine. (a) Top side. (b) Bottom side.

FIGURE 4. Simulation results of coil flux for ψ_{A11}, ψ_{A12}, ψ_{A21} and ψ_{A22}.

TABLE 1. Key design parameters of machine.

Parameters	Quantity
Rated Speed	500 rpm
Rated Torque	35 Nm
Out Diameter	300 mm
Inner Diameter	160 mm
Axial Length	84 mm
Rated Phase Current	100 A (Amplitude)
Phase Resistance	0.015 Ω
Phase Inductance	1.85 mH
Conductor Number	10
Slot Area	962.5 (mm)²
Coil Space Factor	0.5
Current Density in Copper	4.5 A/(mm)²
Conductor Section Area	24 (mm)²

The second complementary characteristic could be verified if the windings besides different PMs are focused. It is demonstrated in Fig. 3(a) that ψ_{A11} and ψ_{A21} is complementary, and in Fig. 3(b), ψ_{A12} and ψ_{A22} is complementary. This characteristic could alleviate the even order harmonics in the final phase flux to ensure the back-EMF has a very sinusoidal waveform. To reveal this dual complementary characteristic, the excitation flux in these four windings is expressed in (1).

$$\begin{cases} \psi_{A11} = \psi_{DCA11} + \displaystyle\sum_{n=1,2,3...}^{+\infty} \psi_{ACA11n}\cos(n\theta_e) \\ \psi_{A12} = -\psi_{DCA11} - \displaystyle\sum_{n=1,2,3...}^{+\infty} \psi_{ACA12n}\cos(n\theta_e + n\pi) \\ \psi_{A21} = -\psi_{DCA21} - \displaystyle\sum_{n=1,2,3...}^{+\infty} \psi_{ACA21n}\cos(n\theta_e + n\pi) \\ \psi_{A22} = \psi_{DCA22} + \displaystyle\sum_{n=1,2,3...}^{+\infty} \psi_{ACA22n}\cos(n\theta_e) \end{cases} \quad (1)$$

where ψ_{DCAij} is the DC component of the ψ_{Aij} and ψ_{ACAijn} is the amplitude of nth harmonics for the ψ_{Aij}. To verify the doubly complementary, the simulation flux for these four windings are presented in Fig. 4. It is shown that the simulation results agree with (1) well, as ψ_{A11} is complementary with ψ_{A12} and ψ_{A21}, ψ_{A22} is complementary with ψ_{A12} and ψ_{A21}. The leakage flux is small which means, it is effective to improve the PM utilization through constructing the complementary structure.

With the design parameters presented in Table 1 that are obtained after robust optimization [22]–[23], a FEA model is built and the electromagnetic performance of the proposed axial-flux machine is evaluated. The total three phase flux is shown in Fig. 5. It is shown that the even old harmonics including the DC complements are alleviated, as the phase flux has a good sinusoidal waveform.

B. HIGH WINDING UTILIZTION FACTOR

The other characteristic of the proposed machine is high winding utilization factor. Because of the special design of the dual complementary structure, the AC component of the excitation flux in four windings belonging to same phase has the same phase position, as shown in Fig. 4. The rotor teeth number is also selected specifically as 11 to construct three phase windings with high winding utilization factor.

Fig. 6 presents the winding flux vectors and winding Back-EMF vectors to demonstrate the high winding utilization factor. Noticeably, the flux vector has DC component, so these flux vectors are divided into two groups, namely the ones with negative DC component, referred as $-F_d$ and with positive DC component, referred as $+F_d$ respectively. The former ones are drawn in the inner circle while the latter ones are drawn in the outer circle. However, the DC component is eliminated when it comes to the Back-EMF vectors. The phase position of the back-EMF in four windings belonging to same phase is totally the same, thus the winding utilization factor of the proposed 12/11 topology is 1, which is
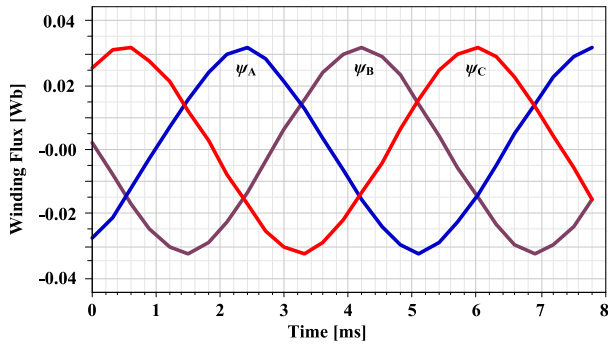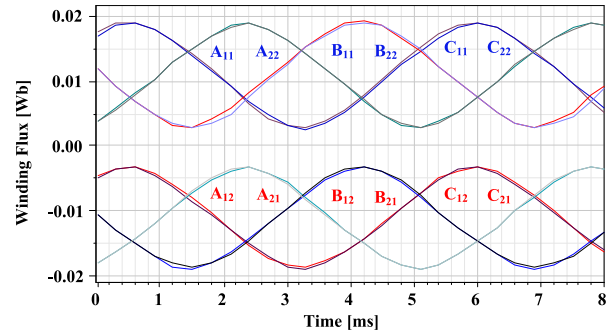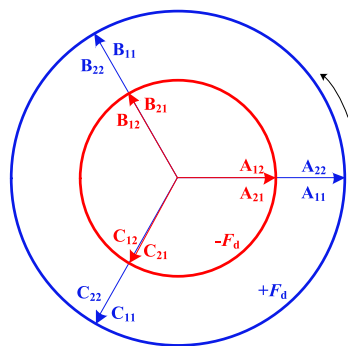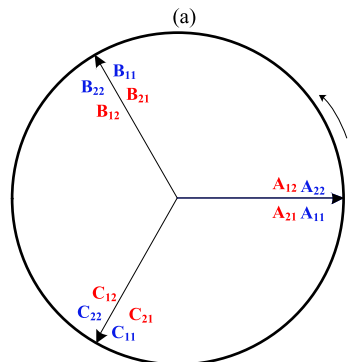
FIGURE 5. Simulation results of three phase flux.

FIGURE 7. Simulation results of the winding flux waveforms.

Winding Flux Vectors

(a)

FIGURE 8. Simulation results of the winding back-EMF waveforms.

Winding Back-EMF Vectors

(b)

FIGURE 6. (a) Winding flux vectors. (b) Winding back-EMF vectors.
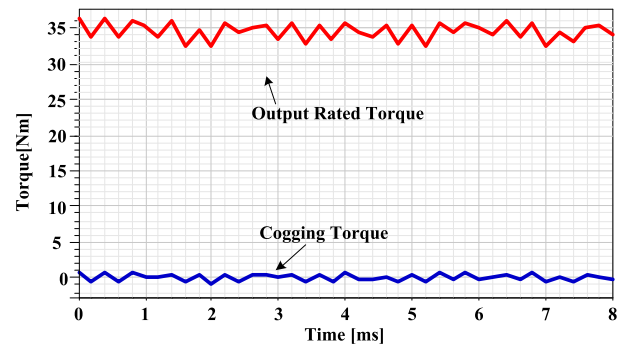
FIGURE 9. Simulation results of the cogging torque.

about 10% higher than that in traditional 12/10 doubly salient PM machine.

Fig. 7 and Fig. 8 give the FEM simulation results of the winding flux and Back-EMF waveforms respectively to verify the analysis above. It is shown the simulation results agree with Fig. 6 well if the high order harmonics are neglected, the winding utilization factor is 1.

C. SMALL COGGING TORQUE

Small cogging torque is another advantage of this proposed machine. This is contributed by the dual complementary structure. Since the excitation flux could switch smoothly between the dual rotors, the rotor will not be stuck at some
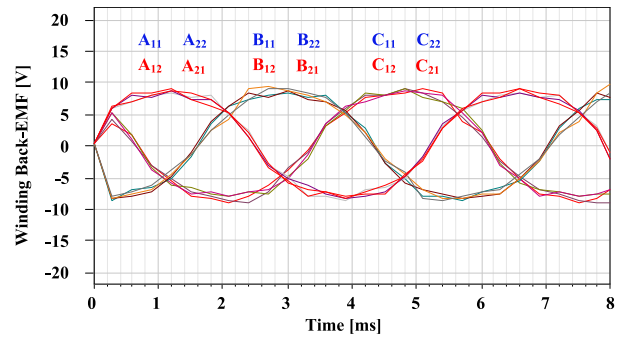
special positions. The cogging torque for this machine is relatively small comparing to the other stator-PM machines with similar double salient structure. Fig. 9 presents the simulation result of the cogging torque and it is shown that the cogging torque only takes about 5.7% of the rated torque, due to its dual complementary structure.

D. INSIGNIFICANT MUTUAL INDUCTANCE

Another important characteristic of this machine is that there is no mutual inductance among different phases. In other words, this machine is combined of three electrically and physically independent single-phase machines. Fig. 10 presents the simulation results of the inductance of phase A, including the self-inductance and the mutual inductance.
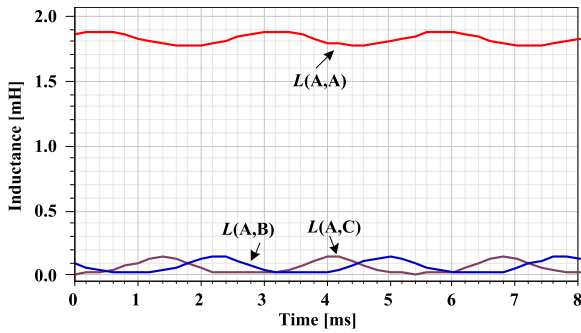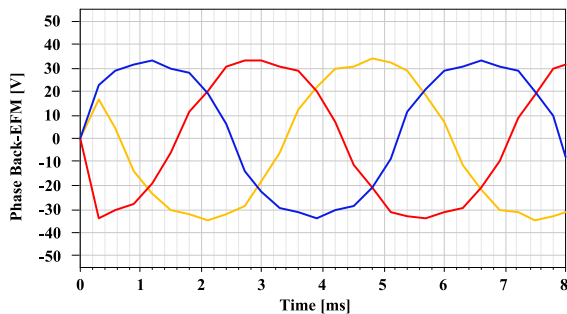
FIGURE 10. Simulation results of the inductances.
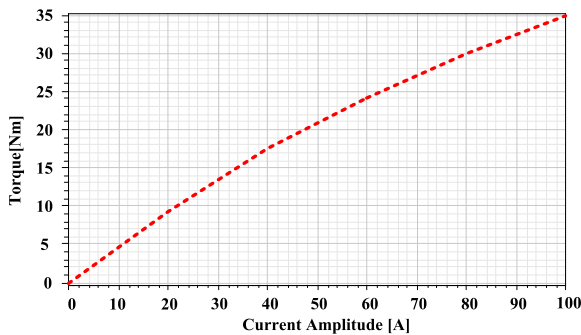

FIGURE 11. Simulation results of three phase back-EMFs.

FIGURE 12. Simulation results of the output torque.

FIGURE 13. Simulation results of the efficiency at rated speed.

FIGURE 14. Radial-flux machine. (a) Side view. (b) Exploded view.

FIGURE 15. Simulation torque of the radial flux motor.

It is seen the self-inductance varies not so much due to the complementary characteristic and the mutual inductance of phase AB and AC is very small when comparing with the self-inductance and can be neglected.

IV. ELECTROMAGNETIC PERFORMANCE AND COMPARITIVE STUDY

A. DUAL COMPLEMENTARY CHARACTERISTICS

Fig. 11 gives the simulation results of the three phase Back-EMFs. It is seen that the waveform is symmetric without even order harmonics, which agrees with the theoretical analysis. Fig. 12 presents the simulation results of the output torque. The torque can reach 35 Nm when the AC amplitude is 100 A. The saturation of the steel is slightly at rated torque, so the torque is not proportional to the current. Fig. 13 gives the efficiency when the machine operating in rated speed with different current. It is shown that the highest efficiency could
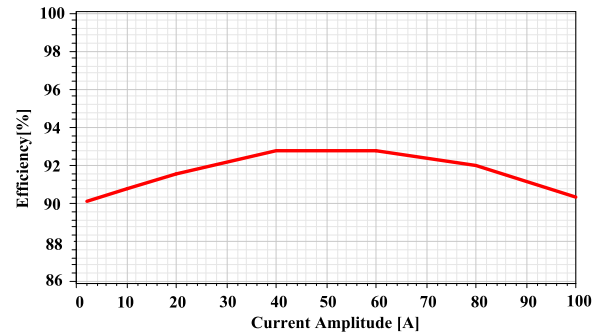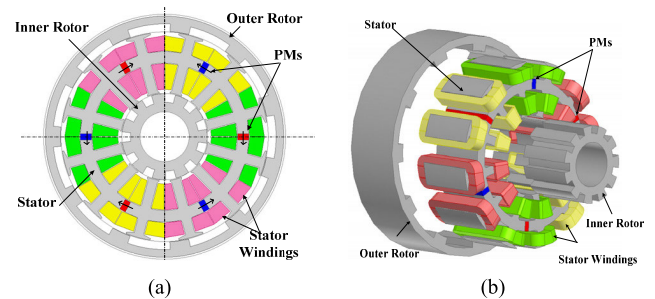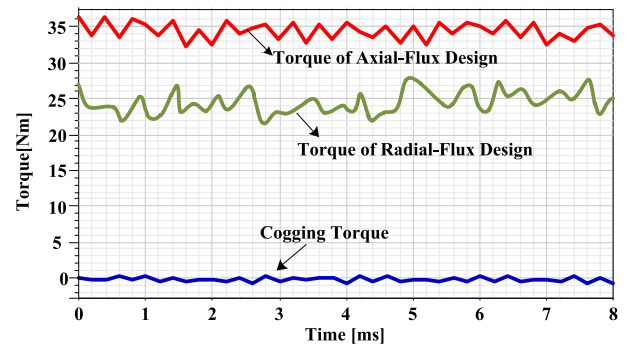
reach 93% and in the whole current range the efficiency is not less than 90%. The power factor in the proposed machine is about 0.65 at rated condition, which is relatively lower than that of traditional PM machines. This is due to strong armature reaction in the proposed machine.

B. COMPARITIVE STUDY

To demonstrate its effectiveness, the proposed axial-flux machine is compared with the radial-flux design which has the same working principle. For comparison, both machines adopt the 12/11 slot/pole topology and are designed based on the same peripheral dimensions and current density. Fig. 14 presents the construction of the radial flux machine including the side view and exploded view of machine. The key design parameters of radial flux machine are presented in Table 2. Fig. 15 shows the simulation result of the torque and cogging torque and it is shown that the torque of 25Nm is

TABLE 2. Key design parameters of radial-flux machine.

Parameters	Quantity
Rated Speed	500 rpm
Rated Torque	35 Nm
Out Diameter	300 mm
Inner Diameter	160 mm
Axial Length	84 mm
Rated Phase Current	120 A (Amplitude)
Conductor Number	10
Slot Area	1154.2 (mm)^2
Coil Space Factor	0.5
Current Density in Copper	4.5 A/(mm)^2
Conductor Section Area	28 (mm)^2

much lower than that in axial-flux machine of 35Nm. This is due to the inner stator of radial flux machine has much smaller inner air-gap diameter than outer air-gap diameter. The calculated rated efficiency for radial and axial flux designs are 84% and 93%, respectively, due to their torque density difference.

V. CONCLUSION

Traditional doubly salient PM machines suffer from the issue of PM open circuit or short circuit circumstances, thus leading to poor PM utilization factor and large torque ripple. Therefore, this paper proposes an axial-flux-complementary doubly salient machine with boosted PM utilization factor for cost-effective direct-drive applications. The proposed machine structure and operation principle are introduced in detail, with its electromagnetic performance verified by 3D time-stepping finite element analysis. Benefiting from the interlaced dual rotor structure as well as the complementary PM magnetic circuit, the proposed machine achieves the boosted PM utilization, eliminated axial force, neglectable cogging torque and thus very low torque ripple, making it a promising candidate for low-cost direct-drive applications such as electric vehicle propulsion.

ACKNOWLEDGMENT

REFERENCES

[1] A. Emadi, Y. J. Lee, and K. Rajashekara, "Power electronics and motor drives in electric, hybrid electric, and plug-in hybrid electric vehicles," *IEEE Trans. Ind. Electron.*, vol. 55, no. 6, pp. 2237–2245, Jun. 2008.

[2] L. Chedot, G. Friedrich, J.-M. Biedinger, and P. Macret, "Integrated starter generator: The need for an optimal design and control approach. Application to a permanent magnet machine," *IEEE Trans. Ind. Electron.*, vol. 43, no. 2, pp. 551–559, Mar. 2007.

[3] Z. Shi, X. Sun, Y. Cai, Z. Yang, G. Lei, Y. Guo, and J. Zhu, "Torque analysis and dynamic performance improvement of a PMSM for EVs by skew angle optimization," *IEEE Trans. Appl. Supercond.*, vol. 29, no. 2, Mar. 2019, Art. no. 0600305.

[4] X. Zhao and S. Niu, "A new slot-PM Vernier reluctance machine with enhanced zero sequence current excitation for electric vehicle propulsion," *IEEE Trans. Ind. Electron.*, to be published.

[5] X. Sun, Z. Shi, G. Lei, Y. Guo, and J. Zhu, "Analysis, design and optimization of a permanent magnet synchronous motor for a campus patrol electric vehicle," *IEEE Trans. Veh. Technol.*, to be published.

[6] B. Zhang, T. Seidler, R. Dierken, and M. Doppelbauer, "Development of a yokeless and segmented armature axial flux machine," *IEEE Trans. Ind. Electron.*, vol. 63, no. 4, pp. 2062–2071, Apr. 2016.

[7] X. Luo, S. Niu, and W. N. Fu, "Design and sensorless control of a novel axial-flux permanent magnet machine for in-wheel applications," *IEEE Trans. Appl. Supercon.*, vol. 26, no. 7, Oct. 2016, Art. no. 0608105.

[8] A. Cavagnino, M. Lazzari, F. Profumo, and A. Tenconi, "A comparison between the axial flux and the radial flux structures for PM synchronous motors," *IEEE Trans. Ind. Appl.*, vol. 38, no. 6, pp. 1517–1524, Nov./Dec. 2002.

[9] X. Zhao and S. Niu, "Design and optimization of a new magnetic-geared pole-changing hybrid excitation machine," *IEEE Trans. Ind. Electron.*, vol. 64, no. 12, pp. 943–952, Dec. 2017.

[10] H. Yang, H. Lin, Z. Q. Zhu, and Y. Liu, "Design and analysis of novel asymmetric-stator-pole flux reversal PM machine," *IEEE Trans. Ind. Electron.*, vol. 67, no. 1, pp. 101–114, Jan. 2020.

[11] X. Zhao and S. Niu, "Design and optimization of a novel slot-PM-assisted variable flux reluctance generator for hybrid electric vehicles," *IEEE Trans. Energy Convers.*, vol. 33, no. 4, pp. 2102–2111, Dec. 2018.

[12] X. Sun, Y. Shen, S. Wang, G. Lei, Z. Yang, and S. Han, "Core losses analysis of a novel 16/10 segmented rotor switched reluctance BSG motor for HEVs using nonlinear lumped parameter equivalent circuit model," *IEEE/ASME Trans. Mechatronics*, vol. 23, no. 2, pp. 747–757, Apr. 2018.

[13] X. Sun, K. Diao, G. Lei, Y. Guo, and J. Zhu, "Study on segmented-rotor switched reluctance motors with different rotor pole numbers for BSG system of hybrid electric vehicles," *IEEE Trans. Veh. Technol.*, vol. 68, no. 6, pp. 5537–5547, Jun. 2019.

[14] H. Yang, H. Lin, Z. Q. Zhu, D. Wang, S. Fang, and Y. Huang, "A variable-flux hybrid-PM switched-flux memory machine for EV/HEV applications," *IEEE Trans. Ind. Appl.*, vol. 52, no. 3, pp. 2203–2214, May/Jun. 2016.

[15] H. Yang, H. Lin, J. Dong, J. Yan, Y. Huang, and S. Fang, "Analysis of a novel switched-flux memory motor employing a time-divisional magnetization strategy," *IEEE Trans. Magn.*, vol. 50, no. 2, pp. 849–852, Feb. 2014.

[16] B. A. R. C. Sekhar and K. R. Rajagopal, "FE analysis of multiphase doubly salient permanent magnet motors," *IEEE Trans. Magn.*, vol. 41, no. 10, pp. 3955–3957, Oct. 2005.

[17] Z. Q. Zhu, Z. Z. Wu, D. J. Evans, and W. Q. Chu, "Novel electrical machines having separate PM excitation stator," *IEEE Trans. Magn.*, vol. 51, no. 4, pp. 1–9, Apr. 2015.

[18] Y. Gong, K. T. Chau, J. Z. Jiang, and W. Li, "Design of doubly salient permanent magnet motors with minimum torque ripple," *IEEE Trans. Magn.*, vol. 45, no. 10, pp. 4704–4707, Oct. 2009.

[19] R. Cao, C. Mi, and M. Cheng, "Quantitative comparison of flux-switching permanent-magnet motors with interior permanent magnet motor for EV, HEV, and PHEV applications," *IEEE Trans. Magn.*, vol. 48, no. 8, pp. 2374–2384, Aug. 2012.

[20] A. Fasolo, L. Alberti, and N. Bianchi, "Performance comparison between switching-flux and IPM machines with rare-earth and ferrite PMs," *IEEE Trans. Ind. Appl.*, vol. 50, no. 6, pp. 3708–3716, Nov./Dec. 2014.

[21] X. Zhao and S. X. Niu, "Design of a novel consequent-pole transverse-flux machine with improved permanent magnet utilization," *IEEE Trans. Magn.*, vol. 53, no. 11, Nov. 2017, Art. no. 8110405.

[22] G. Lei, C. Liu, Y. Li, D. Chen, Y. Guo, and J. Zhu, "Robust design optimization of a high-temperature superconducting linear synchronous motor based on taguchi method," *IEEE Trans. Appl. Supercond.*, vol. 29, no. 2, Mar. 2019, Art. no. 3600206.

[23] X. Sun, C. Hu, G. Lei, Y. Guo, and J. Zhu, "State feedback control for a PM hub motor based on Grey Wolf optimization algorithm," *IEEE Trans. Power Electron.*, to be published.

SHUANGXIA NIU received the B.Sc. and M.Sc. degrees in electrical engineering from Tianjin University, China, in 2002 and 2005, respectively, and the Ph.D. degree in electrical engineering from The University of Hong Kong, Hong Kong, in 2009. She is currently an Associate Professor with the Department of Electrical Engineering, The Hong Kong Polytechnic University, Hong Kong. Her research interests include electrical machines and renewable energy conversion.

XING ZHAO received the B.Sc. degree in electrical engineering from the Department of Automation, Nanjing University of Aeronautics and Astronautics, Nanjing, China, in 2014. He is currently pursuing the Ph.D. degree in electrical engineering with the Department of Electrical Engineering, The Hong Kong Polytechnic University, Hong Kong. His research interest includes novel electrical machines and drives.

TIANTIAN SHENG received the B.S. and M.S. degrees from the Nanjing University of Aeronautics and Astronautics, Nanjing, China, in 2012 and 2015, respectively. He is currently pursuing the Ph.D. degree with the Electrical Engineering Department, The Hong Kong Polytechnic University, Hong Kong. His research interests include stator-PM electric machine, and reluctance machine design and drive.

- - -

XIAODONG ZHANG received the B.Eng. and M.Eng. degrees from the Department of Automation, Tianjin University, China, in 2002 and 2005, respectively, and the Ph.D. degree in electrical engineering from the Department of Electrical and Electronic Engineering, The University of Hong Kong, Hong Kong, in 2011. His research interest includes electric machine design and control.